International Journal of Nanomedicine

Dovepress
open access to scientific and medical research

Open Access Full Text Article

ORIGINAL RESEARCH

Anti-ST2 Nanoparticle Alleviates Lung Inflammation by Targeting ILC2s-CD4$^+$T Response

This article was published in the following Dove Press journal:
International Journal of Nanomedicine

Yumin Wu[1,*]
Weifeng Shi[1,*]
Honghai Wang[2,*]
Jiawei Yue[2]
Yijie Mao[1]
Wei Zhou[1]
Xinagmin Kong[1]
Qiqiong Guo[1]
Lirong Zhang[1]
Pengxiao Xu[1]
Yuyue Wang[1]

[1]Department of Laboratory Medicine, The Third Affiliated Hospital of Soochow University, Changzhou, Jiangsu 213003, People's Republic of China; [2]Department of Orthopaedics, The Third Affiliated Hospital of Soochow University, Changzhou, Jiangsu 213003, People's Republic of China

*These authors contributed equally to this work

Background: Asthma has been regarded as an inflammatory disease, and group 2 innate lymphoid cells (ILC2s) are implicated in asthma pathogenesis. However, no strategy is available to block ILC2s function. Efficiency is also limited due to the use of systemic or subcutaneous routes of administration. The purpose of this study was to investigate the effects of nanoparticles targeting suppression of tumorigenicity 2 (ST2), which is the ILC2 receptor, to alleviate lung inflammation in the murine model of asthma.

Methods: The ultra-small SPIO nanoparticles were firstly synthesized, OVA-induced mice were administered by anti-ST2-conjugated nanoparticles. The inflammatory degree of the lung was investigated by H&E. The percentages of ILC2s and CD4$^+$T cells in bronchoalveolar lavage fluid (BALF) and lung tissue were determined by FACS. Th2-cytokine and OVA-IgE levels were detected by real-time PCR and ELISA, respectively.

Results: Treatment with anti-ST2-conjugated nanoparticles significantly alleviated airway inflammation, IL-33 and IL-13 levels and the percentage of CD4$^+$T cells. The percentage of ILC2s was increased, whereas the levels of IL-13 and IL-5 expressed by ILC2s were reduced.

Conclusion: In the present study, we demonstrated that anti-ST2-conjugated nanoparticles can efficiently control lung inflammation in OVA-induced mice by reducing the ability of ILC2s to produce IL-5 and IL-13, thereby reducing CD4+T cells. Our study also demonstrated that the nanoparticle delivery system could improve the performance of anti-ST2, which may be used as a strategic tool to expand the current drug market.

Keywords: anti-ST2, asthma, group 2 innate lymphoid cells, (ILC2s), CD4$^+$T cells, nanoparticle

Introduction

Asthma is one of the most common respiratory diseases, which has affected more than 300 million people worldwide, and it is associated with a large socioeconomic burden.[1] As many other immune-mediated diseases, asthma develops as a result of interaction between exposure to external risk factors and alterations in specific pathways of the immune network.[2] Currently, two types of asthma are defined by their different cellular and molecular phenotypes: "high type 2 (T2) immunity asthma" and "low type 2 immunity asthma". "Low type 2 immunity asthma" is also known as "noneosinophilic asthma" and is associated with neutrophilic or IL-17-driven airway inflammation. "High type 2 immunity asthma" is noted in approximately 50% of asthmatic patients and is characterized by a high Th2 response as well as peripheral eosinophilia.[3] The most common molecular mechanism responsible for the pathogenesis of T2 immunity asthma is activation of the T2

Correspondence:Yuyue Wang
The Third Affiliated Hospital of Soochow University, Changzhou, Jiangsu213003, People's Republic of China
Email wangyuyue1085@126.com

submit your manuscript | www.dovepress.com
DovePress
http://doi.org/10.2147/IJN.S268282

inflammatory pathway, which is characterized by elevated T2 cells (Th2 and group 2 innate lymphoid cells (ILC2s)) and T2 cytokines (IL-4, IL-5, IL-9 and IL-13).[4]

Despite optimal guideline-directed treatment, patients with asthma experience exacerbations, which are caused by an accentuation of existing inflammatory processes and a loss of disease control. Thus, alternative therapeutic approaches that better control the progress of asthma are urgently needed. Biologic therapy has yielded dramatic results in the treatment of dermatologic, rheumatologic and gastroenteric diseases, and a role for biologic therapy in the treatment of asthma has been recently reported as well.[5] Biologic drugs used in asthma include monoclonal antibodies, which can block pro-inflammatory cellular pathways. Some targets have been used to block Th2-pathway cytokines, such as the IL-4 and IL-13 receptor (dupilumab), IL-5 (mepolizumab and reslizumab) or its receptor (benralizumab) and IgEs (omalizumab).[5] Traditionally, Th2-pathway cytokines are the believed to be the principal drivers of T2 inflammatory conditions. However, recent studies have suggested that ILC2s seemed to play a more critical role in asthma. ILC2s produce significant amounts of IL-13, IL-5, IL-9 and IL-4 in response to IL-33, IL-25 and thymic stromal lymphopoietin (TSLP) produced by epithelial cells. Thus, we aim to identify effective targets that block the ILC2 pathway in asthma.

ILC2s are members of innate lymphoid cells (ILCs), which can be divided into four subsets corresponding to various innate populations that are characterized by their production of type 1-, type 2-, type 17- and Treg-associated cytokines, respectively. LC2s are characterized by the lack of lineage-defining cell surface markers (Lin^-) and express CD45, IL-33R (ST2), IL-17RB (a component of the IL-25R), ICOS (CD278), and Thy1; these cells been has been described in gut, lungs, skins, BALF and peripheral blood.[6] ILC2s produce significant amounts of IL-13, IL-5, IL-9 and IL-4 in response to IL-33, IL-25 and thymic stromal lymphopoietin (TSLP). Of note, the ability of IL-33 to activate ILC2s is 1000-fold greater than the other two cytokines.[7] As a source of IL-13, ILC2s are required for the expulsion of intestinal helminths, allergy and airway inflammation and homeostasis.[7] A previous study reported that in the absence of IL-33, ILC2 responses were significantly diminished, whereas delivery of exogenous IL-33 enhanced ILC2 responses.[8] IL-33 exerts its dramatic effects via ST2 expression on ILC2s. Thus, we hypothesized that we can block the IL-33/ILC2s axis by specifically blocking ST2 on ILC2s as a new novel biologic therapy. However, the main limiting factor of this approach is the route which used for antibody administration.

The efficiency of aerosol antibodies delivering to the lung has been limited due to the active clearance in the lungs, which markedly reduce the antibodies' residence duration and tissue penetration. Novel nanosized carriers may be an option to overcome these limitations, providing a promising method for the efficiently delivering blocking antibodies which directly to asthmatic lungs.[9] This approach improves the sensitivity and tissue penetration of nanoparticles (NPs) by optimizing their composition, size, and structure. Among many available nanoparticles, ultra-small SPIO (superparamagnetic iron oxide) nanoparticles have aroused wide interest for their low intrinsic toxicity, easy surface functionalization, easy coupling to target groups and easy detection. These properties have offered new prospects for novel magnetic nanoparticles that can improve treatment and diagnosis in a unique multifunctional system.[10] In this paper, we demonstrate that DiR-SPION conjugated to anti-ST2 blocking antibodies (anti-ST2 NPs) efficiently suppressed the development of asthma by block the function of ILC2s.

Patients and Methods

Patients

The study was conducted in accordance with the principles of the Declaration of Helsinki and conducted in the Third Affiliated Hospital of Soochow University (Changzhou, China) and reviewed and approved by the ethical committee of the Third Affiliated Hospital of Soochow University (Changzhou, China). Written informed consent of the younger children was obtained from the parents. Thirty asthmatic children and thirty healthy control were recruited from our outpatient clinic who were diagnosed based on commonly accepted guidelines. None of the subjects received treatment at the time of blood collection. They were excluded from our study when they had a history of atopic dermatitis, allergic rhinoconjunctivitis, or autoimmune disease. In addition, when they had an acute infection during the previous 2 weeks, current C-reactive protein elevation, clinical symptoms of a current infection, or leukocytosis, they were also excluded.

Characterization of SPIO-Anti-ST2 Nanoparticles

The ultra-small SPIO nanoparticles were firstly synthesized according to the literature reported protocol.[11] Generally, 4 mmol ferric acetylacetonate (Sigma-Aldrich) and 20 mmol 1, 2-Hexadecanediol (Sigma-Aldrich) were dissolved in a mixture of 12 mmol oleic acid (OA, Sigma-Aldrich), 12 mmol oleylamine (OM, Sigma-Aldrich) and 40 mL benzyl ether (Sigma-Aldrich) and magnetically stirred under the flow of nitrogen. The mixture was then heated to 200 °C for 2 h, and further heated to 300 °C for 1 h. After cooling down to the room temperature, the product was precipitated and washed with ethanol for several times. Finally, The OA capped SPIO nanoparticles were redispersed in chloroform for further use. The yielded SPIO nanoparticles were then modified with a kind of amphipathic polymer, polyethylene glycol-conjugated 1,2-distearoyl-sn-glycero-3-phosphoethanolamine-maleimide (DSPE-PEG-MAL) (Avanti Polar Lipids, Inc.), via the hydrophobic interaction. Briefly, DSPE-PEG-MAL and DSPE-PEG at a mass ratio of 1:1 (30 mg in chloroform) was dropwisely added into SPION solution (6 mg in chloroform) under sonication. After stirring at room temperature overnight, the chloroform was removed by using a rotary evaporator. The obtained SPIO-PEG-MAL nanoparticles were redispersed in PBS for further use.

To conjugate the thiolated ST2 monoclonal antibody (Abcam, CA, USA) on the SPIO-PEG-MAL nanoparticles as well as the isotype antibody anti-IgG, 13.4 μg of anti-ST2 and anti-IgG was mixed with 1 mg of SPIO-PEG-MAL nanoparticles, respectively, and then stirred at room temperature for 24 h. The nanoparticles were purified by using gel filtration chromatography (Sephadex^{TM} G-100, Sigma-Aldrich) to remove the excess ST2. DiR (1, 1′-dioctadecyltetramethyl indotricarbocyanine iodide) was loaded into the hydrophobic layer of SPIO-anti-ST2 and SPIO-anti-IgG nanoparticles.

The polydispersity index (PDI) of nanoparticles before and after their conjugation with ST2-NPs was measured on a Nano-ZS90 zetasizer (Malvern, UK). Nanoparticles were analyzed at an iron concentration range of 0.01–1 mg/mL in different solutions, and the average of three measurements was taken. The coupling efficacy of anti-ST2 and anti-IgG on the nanoparticles was determined by measuring the amounts of residue proteins in the supernatants and the amounts of added proteins using a Pierce BCA Protein Assay kit (Thermo Scientific) after which protein was stored at −4°C for further study.

Mice

Female Balb/c mice (4 weeks old, 18–20 g), were purchased from the laboratory animal center of Soochow University (Suzhou, China) and maintained in the Soochow University Animal Center (Jiangsu, China). All animal experiments were approved by the Soochow University Animal Ethics and Experimentation Committee and followed the guidelines for the ethical review of laboratory animal welfare People's Republic of China National Standard GB/T 35892-2018 which issued 6 February 2018 effective from 1 September 2018.[12] Mice were separated into 6 groups (10 mice in each group): PBS, OVA, PBS + anti-IgG-NPs, OVA + anti-IgG-NPs, OVA + anti-ST2, and OVA + anti-ST2-NPs. The mice were actively sensitized through intra-peritoneal (i.p.) injections of 100 μg of ovalbumin (OVA) (Bio Basic, Markham, ON, Canada) and 2 mg of Alum (AlumImject; Pierce, IL, USA) in 100 μL of phosphate-buffered saline on day 1 and day 11. Then mice were inhaled with 2% OVA by nebulization using a atomizer (Omron, Japan) for 3 consecutive days from day 22. Mice were intrapulmonary instilled with either PBS, anti-ST2, anti-IgG1-NPs or anti-ST2-NPs (Figure 1A) on days 19, 20 and 21 using a MicroSprayer aerosolizer (Penn-Century Inc., PA, USA). The dose of all antibody-NPs corresponds to 1 mg iron oxide per kg of body weight. Anti-ST2 antibody was administered at 0.3 μg per mouse (that is, 15 μg.kg - 1), which amount corresponds to the conjugated antibody in the iron oxide nanoparticles. Mice in the non-sensitized group were given or not given anti-IgG1-NPs at the same time interval. Combined with H&E staining, nanoparticles were confirmed successfully target inflammatory lung tissue in vivo, FACS detection of DiR in DiR-conjugated anti-ST2-NPs. On day 26, all the mice were sacrificed and BALF and lungs were collected from all groups of mice.

Cell Preparation and Flow Cytometric Quantification

Peripheral blood mononuclear cells (PBMCs) from human and mice were obtained by Ficoll-Hypaque density-gradient centrifugation and divided into two equal parts, one of which was immediately used for flow cytometry, and then added 1 mL Trizol (Invitrogen, USA) into the other aliquots and was stored at −80°C for extracting total RNA. Mice lung and BALF samples were collected from all groups of mice. For flow cytometric quantification, single-cell suspensions were then stained with flowing fluorescence

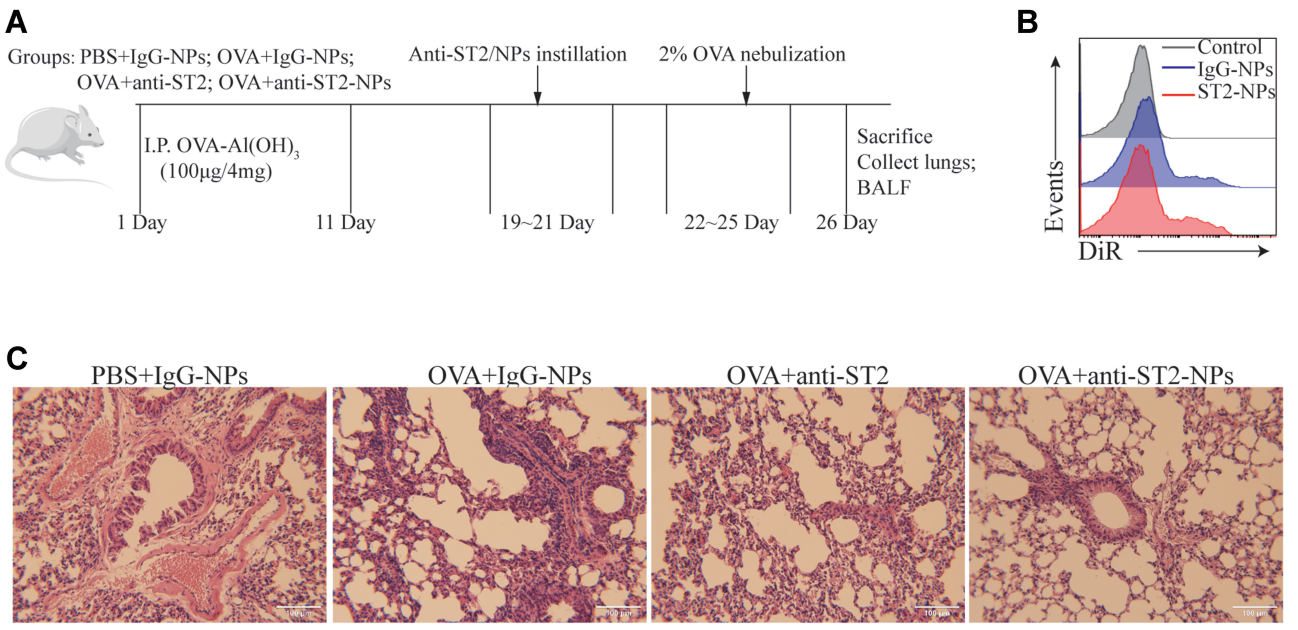

Figure 1 Airway inflammation was alleviated by anti-ST2-NPs. (**A**) On the basis of establishing asthma model, the mice were treated with anti-ST2 and anti-ST2-NPs, respectively. (**B**) Flow cytometry evaluated the expression of DiR in lung. (**C**) Lung tissue sections of different groups of mice were stained with H&E.

conjugated different monoclonal antibodies: anti-Lineage (CD2, CD3, CD14, CD16, CD19, CD56, and CD235a, eBioscience, San Diego, CA, USA), anti-CD90.2, anti-ST2, anti-KLRG1 (R&D Systems, Inc., Minneapolis, MN, USA). Intracellular staining for IL-5 and IL-13 (eBioscience, San Diego, CA, US) was performed with the Cytofix/Cytoperm kit (BD Biosciences) after 3 hr restimulation of 1×10^5 total cells in 500 mL RPMI-1640 media containing 10% FBS, Penicillin/Streptomycin (P+S), 2-mercaptoethanol (2-ME), Brefeldin A (GolgiPlug, BD Biosciences), PMA (30 ng/mL), and ionomycin (500 ng/mL) at 37 °C. For human ILC2s cell detection, cells were triple stained with anti-Lineage, anti-CD127, anti-IL-CRTH2 mAbs (R&D Systems, Inc., Minneapolis, MN, USA) according to the manufacturer's instructions. The labeled cells were quantified on a LSRII flow cytometer (BD, Franklin Lakes, NJ) and analyzed using FlowJo software (vX.0.7, Tree Star, Ashland, OR).

Isolation of ILC2s and Cell Viability Assay

ILC2s were sorted by magnetic beads combined with flow cytometry from mice spleen. Mice splenic cell suspension was stained by Biotinbinding antibodies (anti-CD21/CD35, anti-Ter-119, anti-CD45R, antiCD3, anti-CD11b, and anti-CD49) (Miltenyi Biotec, Belgish-Gladbach, Germany), and then combined with Streptavidin-MicroBeads, the negative cells were enriched by magnetic column. This step was mainly to remove most of the lineage-expressing cells in spleen, thus enriching lineage-negative cells. The enriched cells were stained with FITC-lineage (eBioscience, San Diego, CA, USA), PE-CD90.2, and APC-ST2 (R&D Systems, Inc., Minneapolis, MN, USA), then further sorted by flow cytometry. The sorted cells (1×10^5 cells per well in a 96-well plate) were cultured in 1640 medium supplemented with 10% FBS, 10 ng/mL IL-7, 10 ng/mL IL-2, and10 ng/mL IL-33 (Peprotech, Rocky Hill, USA), 10 U/mL Penicillin and 10 U/mL streptomycin. Three days later, ILC2s were cultured with IgG-NPs at 0, 2, 4, 8 and 16μg/mL for 24h and 48 h. The cell viability was determined using cell counting kit (CCK8) (Dojindo, Japan) according to the manufacturer's instructions. The plates were scanned at 450 nm for absorbance using a spectrophotometer (BioTek, Winooski, VT, USA). Each data point was measured for the average from six duplicates. The experiments were repeated independently for 3 times.

RNA Isolation and Real-Time Quantitative PCR

Human PBMCs and mice lung tissues as well as mice BALF supernatants were homogenized in Trizol reagent (Invitrogen, Carlsbad, CA). Total RNA was extracted from cells and tissues using Trizol reagent according to the manufacturer's instructions, and equal amount of RNA was used for RT-PCR and real-time RT-PCR analyses. *β-actin* was used as an internal control. The following primers were

sequences utilized. h-*β*-actin:5′-TGGCACCCAGCAC AATGAA-3′ (forward), 5′- CTAAGTCATAGTCC GCCTAGAAGCA-3′ (reverse); h*IL-33*:5′- TGACGGTG TTGATGGTAAGATG-3′ (forward), 5′-ACAGAGTGTTC CTTGTTGTTGG-3′ (reverse); h*IL-13*:5′- GGCTGAGGT CTAAGCTAAGG -3′ (forward), 5′- GACAGCTGGCAT GTACTGTG -3′ (reverse); and h*IL-5*:5′- ACTCTCCAG TGTGCCTATTC -3′ (forward), 5′- CTGCTGATAGCCAA TGAGAC-3′ (reverse); h*ST2*:5′- AGATGAGTCACTGGC ATACG -3′ (forward), 5′- GAGAGGCTGGCTGTTGTA TT -3′ (reverse); m-*β*-actin:5′- TGGAATCCTGTGGCATTC ATGAAAC

-3′ (forward), 5′- TAAAACGCAGCTCAGTAACAGT CCG -3′ (reverse); mIL-33:5′- TAAAACGCAGCTCAGT AACAGTCCG-3′ (forward), 5′- TAAAACGCAGCTCAG TAACAGTCCG-3′ (reverse); m*IL-13*:5′- TGAGCAACAT CACACAAGACC-3′ (forward), 5′- AGGCCATGCAATA TCCTCTG -3′ (reverse); and m*IL-5*:5′- AGGCCATGCAA TATCCTCTG -3′ (forward), 5′- CCTCATCGTCTCATTG CTTG-3′ (reverse); m*ST2*:5′- TGGACAGCACCTGTTCA GT-3′ (forward), 5′- CAGGACATCAGCCAAGAAGT −3′ (reverse); The relative mRNA expression quantification was calculated with the comparative threshold cycle (Ct) method.

Histological Examination

The left lungs were removed, fixed in 4% paraformaldehyde, dehydrated and embedded in paraffin. The tissue was cut into 4-μm-thick sections and stained with hematoxylin and eosin (H&E) for evaluation of inflammation. Inflammation in H&E-stained lung sections was evaluated with a subjective score ranging from 0 to 5 by five independent, blinded readers according to a semiquantitative scoring system[13] as mild (score 1–2), moderate (score 3), or severe (score 4). Briefly, this score was described as the following categories: no inflammation: 0; few inflammatory cells: 1; a ring of inflammatory cells 1 cell layer deep: 2; a ring of inflammatory cells 2–4 cells deep: 3; a ring of inflammatory cells >4 cells deep: 4. Lung sections of each group were counted, and at least 1000 epithelial cells were analyzed in each section. The results were calculated as the percentage of positive cells in each group. Data are presented as medians (range). All experiments were performed in three times.

Statistical Analysis

All statistical analyses were performed using Prism 5 (Graph Pad Software, La Jolla, CA, USA). Data were expressed as the mean ± SD. Statistical comparisons between groups were performed using Student's unpaired *t*-test. Spearman's test was used for correlations between two continuous variables. Differences were statistically significant when p-values were 0.05 or less.

Results

Circulating Baseline Characteristics in Patients with Asthma

Thirty asthmatic children and thirty healthy controls between 4 and 18 years of age were included in this study. Peripheral blood baseline characteristics are shown in Table 1. The male-to-female ratio was 12:18. The mean age of the asthmatic group was 7 ± 2.7 years old, and the mean age of control group was 7 ± 2.15 years old. Peripheral leukocytes, eosinophil and neutrophil counts in asthmatic group were significantly increased compared with the control group.

ILC2s are Significantly Correlated with Increased ST2 Expression

We examined the relative and absolute numbers of ILC2s in the peripheral blood. Human ILC2s were defined as $Lin^{+}CD127^{+}CRTH2^{+}$ cells (Figure 2A). We observed that ILC2 frequencies were significantly increased in asthma patients ($P < 0.001$) compared with that in healthy controls (Figure 2B). We also detected the expression of ST2, and our results showed a similar tendency consistent with ILC2s (Figure 2C). Similar results were found in IL-33, IL-13 and IL-5 mRNA levels (Figure 2D–F). A significant positive correlation was identified between ST2 levels and ILC2 frequencies in asthma patients ($P < 0.05$; Figure 2H). No significant correlation was found between ST2 and patient age and the amount of leukocytes (Figure 2H and G).

Elicitation of an ILC2-$CD4^{+}$T Response Following OVA-Induced Asthma

We and other teams have previously confirmed that ILC2s constitutively populate in human and murine lung, and ILC2 cell numbers and effector cytokines are elevated in the context of asthma, demonstrating that ILC2s promote asthma development. In this study, we sought to examine whether an ILC2 response was induced in our experiment. Mice were exposed to OVA as described in Figure 3A. Increased numbers of infiltrating inflammatory cells near submucosal layers and airway remodeling/collagen deposition were observed in OVA-treated mice (Figure 3B). Flow cytometry showed that direct airway challenge of OVA-sensitized mice with OVA caused robust elevation of ILC2 numbers in bronchoalveolar

lavage fluid (BALF) (Figure 3C and D). The total number of ILC2s was also elevated relative to PBS control-challenged animals in the lung tissue of OVA-challenged mice (Figure 3E and F). Significantly elevated ST2 levels were also found in OVA-challenged mice in lung tissue (Figure 3G). RT-PCR analysis showed significantly elevated IL-33 concentrations in the lung parenchyma in OVA-challenged mice relative to control PBS challenge, and the expression of IL-13, IL-5 and IL-4, which are significant cytokines produced by activated ILC2s, were also increased (Figure 4A–D). We then analyzed the concentration of specific OVA-IgE in BALF. Elevated OVA-IgE levels were found in OVA-challenged mice (Figure 4E), and we also observed a positive correlation with elevated ST2 and ILC2s (Figure 4F and G).

Animals challenged with OVA exhibited a significantly elevated percentage of CD4+T cells in lung tissue (Figure 4H and I). The tendency was significant correlated with ILC2s (Figure 4J).

DiR-SPIO-ST2-NP Characterization

The TEM image and size distribution of DiR-SPIO-ST2-NPs are shown in Figure 5. DiR-SPIO-ST2-NPs has a uniform size and PDI (Figure 5C, Supplementary Table 1). TEM images indicated that the DiR-SPIO-NPs were core-shell spherical nanoparticles (Figure 5A and B). The stability of SPIONs in different media was assessed by monitoring the size distribution for 48 h, revealing excellent stability for all formulations before and after antibody conjugations (Figure 5D, Supplementary Table 2). The combining efficiency of SPIO-anti-ST2 and SPIO-anti-IgG nanoparticles were 82.76% and 83.53%, respectively. Before conducting the related experiments, we studied in vitro cytotoxicity via the standard cell viability CCK8 assay for ILC2s. It was found that SPIO-anti-IgG NPs exhibited little toxicity to cells even under high concentrations after 48 hours of incubation (Supplementary Figure 1).

Table 1 Characteristics of the Study Population

Characteristics	Asthma	Control	*p*
Number	30	30	ns
Age (years) (mean ± SD)	7 ± 2.7	7 ± 2.15	ns
Sex, female/male	12/18	17/13	ns
Peripheral leukocytes (/μL)	8.2 ± 1.41	5.4 ± 1.21	<0.05
Peripheral eosinophils (/μL)	349.6 ± 203.65	207.4 ± 127.39	<0.05
Peripheral neutrophils (/μL)	4095.7 ± 1078.35	3344.2 ± 673.35	<0.05

Airway Inflammation Was Alleviated by Anti-ST2-NPs

To investigate whether ST2 signaling blockade contributes to the development of airway inflammation, anti-ST2 antibodies and anti-ST2-NPs were administered to OVA-induced mice, and the procedure is presented in Figure 1A. To detect the efficient delivery of nanoparticles, the localization of the instilled anti-ST2-NPs in inflammatory lung tissues was confirmed by FACS to examined the DiR-labeled anti-ST2-NPs (Figure 1B). As expected, anti-ST2-NPs efficiently localized within the areas of lung tissues of OVA-induced mice treated with anti-ST2-NPs (Figure 1B).

In the present study, we found a marked decrease in inflammation in OVA-induced mice treated with anti-ST2 compared with OVA-induced mice, and the alleviation was more remarkable when mice were treated with anti-ST2-NPs (Figure 1C).

ILC2s Were Elevated in Lung Tissue After Treated with Anti-ST2-NPs

ILC2s are major players during asthma and are the main cells expressing ST2. Interestingly, a noteworthy increase in ILC2s was found in OVA-induced mice treated with anti-ST2 and anti-ST2-NPs (Figure 6A and B); however, remarkable decreases in IL-33 (Figure 6C) and IL-13 (Figure 6D) were contradictorily found in OVA-induced mice treated with anti-ST2 and anti-ST2-NPs compared with OVA-induced mice.

Airway Inflammation is Alleviated by Anti-ST2-NPs That Target the ILC2s-CD4+T Axis

To explain the inconsistent association of ILC2s with IL-33 and IL-13, we next examine the percentage of $CD4^+$T cells in the lung tissue. Consistent with our conjecture, reduced $CD4^+$T cells were found in OVA-induced mice treated with anti-ST2-NPs compared with OVA-induced mice (Figure 7A and B). Next, we assessed functional cytokines secreted by ILC2s to determine ILC2 activity. As expected, we found that IL-13 and IL-5 production was distinctly repressed by anti-ST2-NPs in vivo (Figure 7C and D), potentially affecting the promotion of $CD4^+$T cells by ILC2s.

Discussion

Several clinical and experimental studies have indicated the critical role of ILC2s and the receptor ST2, which

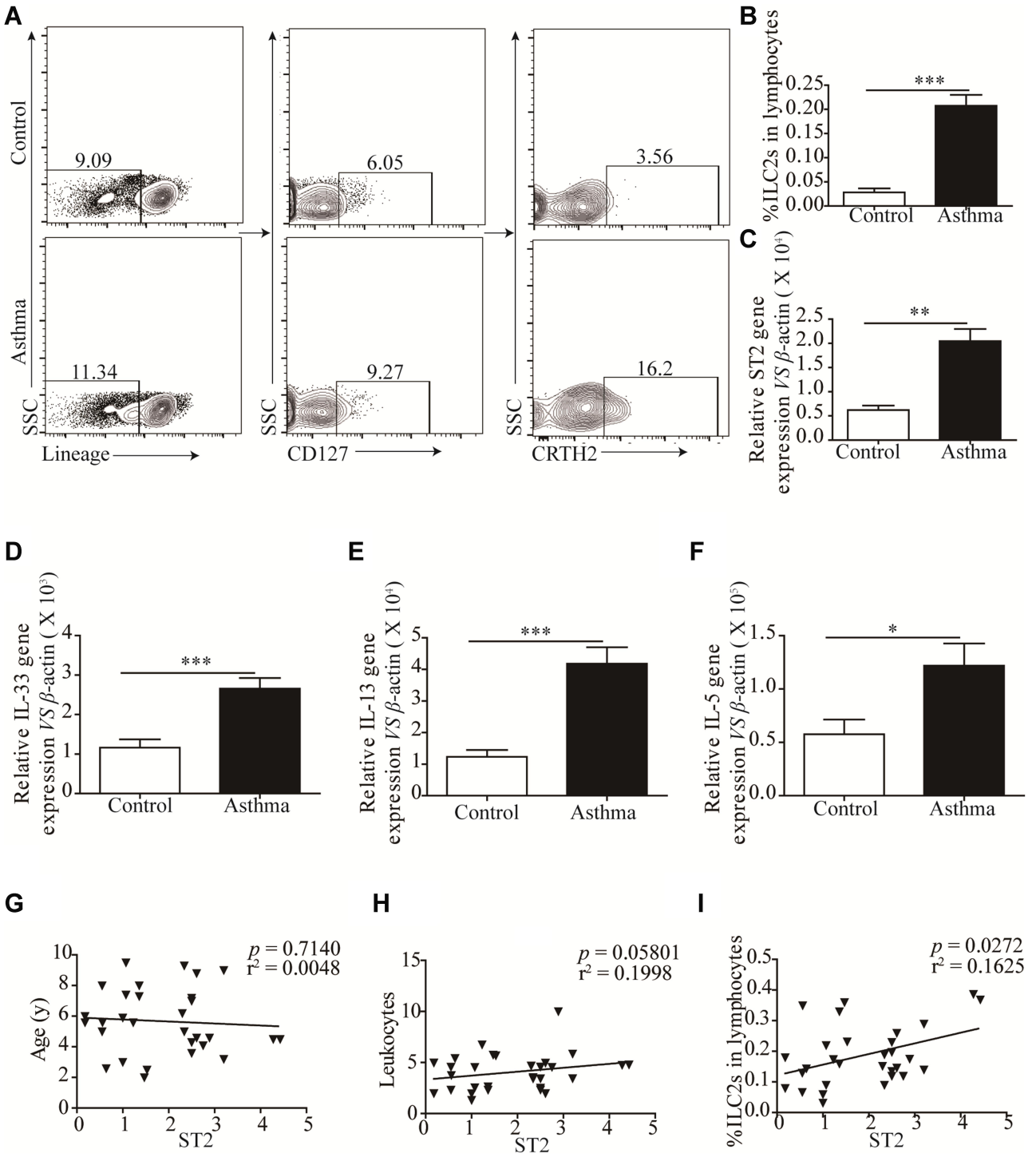

Figure 2 Significantly Increased ILC2s is correlated with elevated ST2. (**A** and **B**) Representative flow cytometry plots and corresponding quantitation of circulating $Lin^{-}CD127^{+}CRTH^{+}$ ILC2s in health control and asthmatic patients. Representative diagrams of the mRNA levels of ST2 (**C**), IL-33 (**D**), IL-13 (**E**) and IL-5 (**F**) in health control and asthmatic patients. No correlation was found between ST2 with patients' age (**G**) and the number of leukocytes (**H**), significant positive correlation was found between ST2 and the percentage of ILC2s in asthmatic patients (**I**). ***p<0.001; **p<0.01; *p<0.05.

expressed in ILC2s and some other immune cells, in the development of airway inflammation.[14] Further, ILC2s has also been suggested as the therapeutic target of asthma treatment.[15] Considering this information, we hypothesized that airway inflammation can be alleviated by blocking ST2.

We first detected the percentage of ILC2s in asthmatic patients and healthy controls. Our results showed elevated

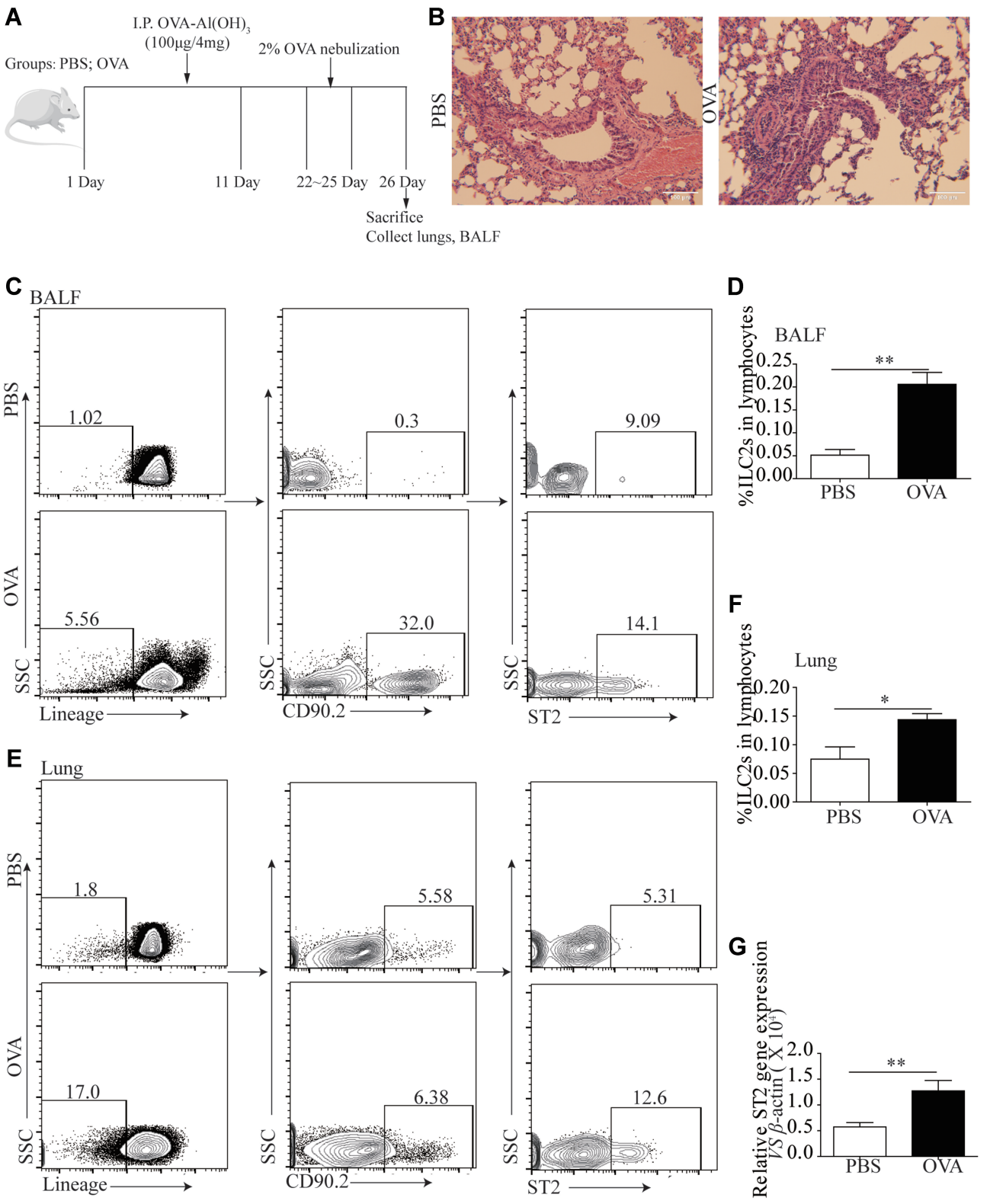

Figure 3 ILC2s and ST2 was elevated following OVA-induced asthma. A cohort of Balb/c mice were either induced with PBS or OVA by intraperitoneal injections and four days according to the scheme, n = 8. (**B**) H&E staining was performed on PBS and OVA treated mice lung tissue sections. (**C**) Representative diagrams of flow cytometry analysis of the percentages of ILC2s in the BALF of OVA and PBS treated mice. (**D**) Frequencies (n = 8) of percentage of ILC2s in mice BALF. (**E**) Representative diagrams of flow cytometry analysis of the percentages of ILC2s in the lung of OVA and PBS treated mice. (**F**) Frequencies (n = 8) of percentage of ILC2s in mice lung. (**G**) RT-PCR results of the relative expression of ST2 in mice lung tissue. Data are presented as mean ± SD, *P < 0.05; **P < 0.01 compared with control.

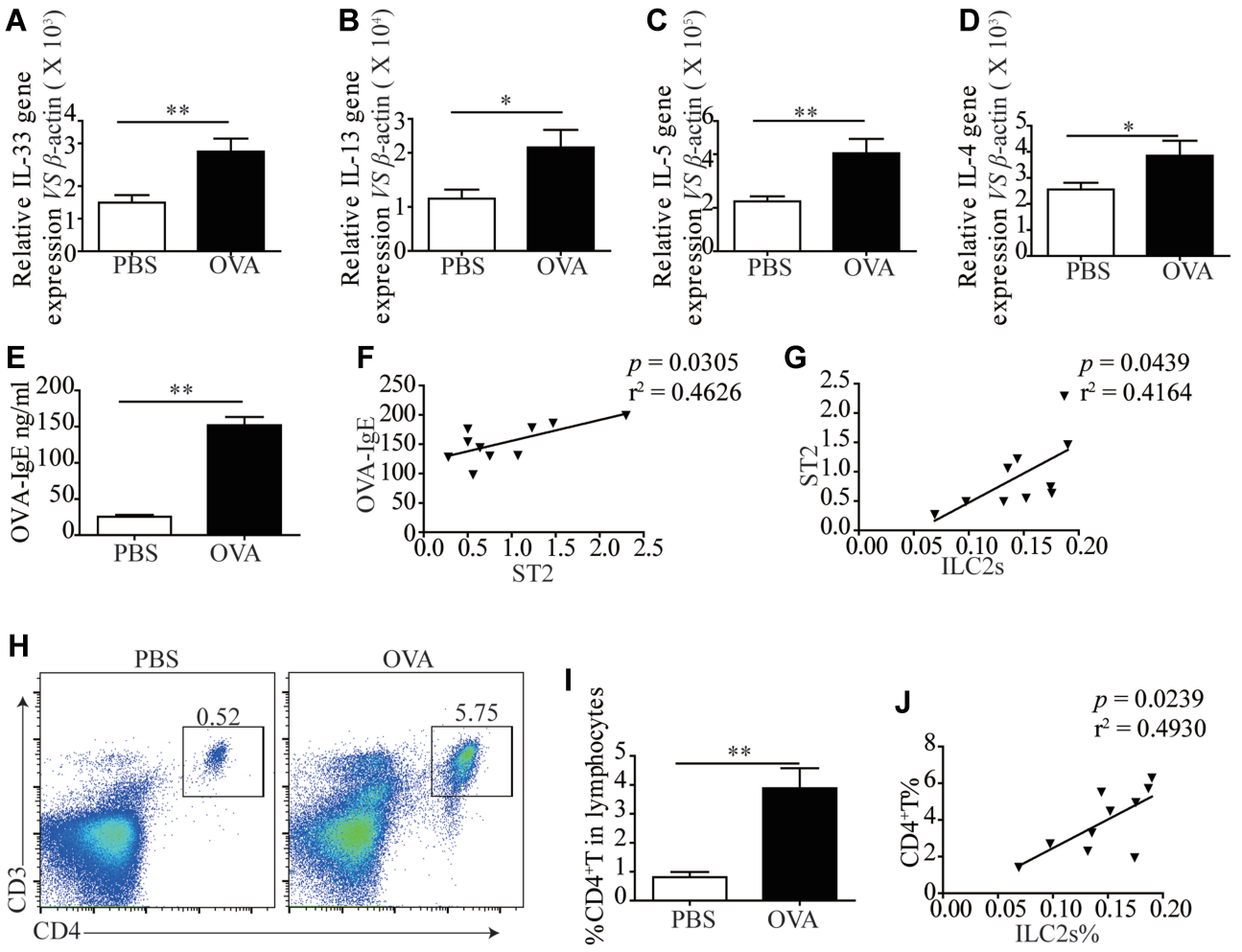

Figure 4 Elevated ILC2s related cytokines and elicitation of $CD4^+T$ response following OVA-induced asthma. RT-PCR results of the relative expression of IL-33 (**A**), IL-13 (**B**), IL-5 (**C**) and IL-4 (**D**) in mice lung tissue. (**E**) ELISA results showed more OVA-IgE in the BALF of OVA treated mice than PBS treated mice. (**F**) The correlation of OVA-IgE and ST2 mRNA expression ($P = 0.0305$, $r^2 = 0.4626$). (**G**) The correlation of ILC2s% and ST2 mRNA expression ($P = 0.0439$, $r^2 = 0.4164$). (**H**) Representative examples of flow cytometry analysis of $CD4^+T$ cells percentage in PBS and OVA treated mice lung. (**I**) Frequencies (n = 8) of percentage of $CD4^+T$ cells in mice lung. (**J**) The correlation of ILC2s% and $CD4^+T$% ($P = 0.0239$, $r^2 = 0.4930$). Data are presented as mean ± SD, *P < 0.05; **P < 0.01 compared with control.

ILC2s and related cytokines IL-33, IL-13 and IL-5 in PBMC of asthmatic patients compared with healthy controls, and ILC2 levels were significantly correlated with elevated ST2 levels (Figure 2). However, no significant correlation was found between ST2 and patient age and the amount of leukocytes (Figure 2G and H). This finding may indicate that elevated ST2 in asthmatic patients mainly correlated with elevated ILC2s. ILC2s promote the development of several inflammatory diseases, such as nasal polyp, allergic rhinitis, and parasitic infection.[15] Moreover, numerous studies from others and us have demonstrated that ILC2s were elevated in asthmatic patients and execute their function mainly by secreting IL-13, IL-5 and IL-4 when activated by IL-33, IL-25 and TSLP.[16,17] Studies have found that IL-33 activates ILC2s 1000~fold more effectively than IL-25 and TSLP, and IL-33-activated ILC2s exhibit increased ST2 expression.[7]

To illustrate the possibility of alleviating airway inflammation by blocking ST2, we next constructed an asthma model via OVA induction. As shown in Figure 3, we observed an increase in the total numbers of inflammatory cells in the airway of OVA-induced mice compared to naïve controls, which is similar to previous results. Our OVA mouse model of allergic asthma also generated a reaction that caused ILC2 infiltration in BALF and lung tissue (Figure 3C–F). We also detected ST2 expression in lung tissue and found increased ST2 expression levels that were similar to increases in ILC2s (Figure 3G) and its ligand IL-33 (Figure 4A). Concomitantly, changes also occurred in IL-13, IL-5 and IL-4, indicating that our OVA mouse model recapitulated changes in asthmatic patients.

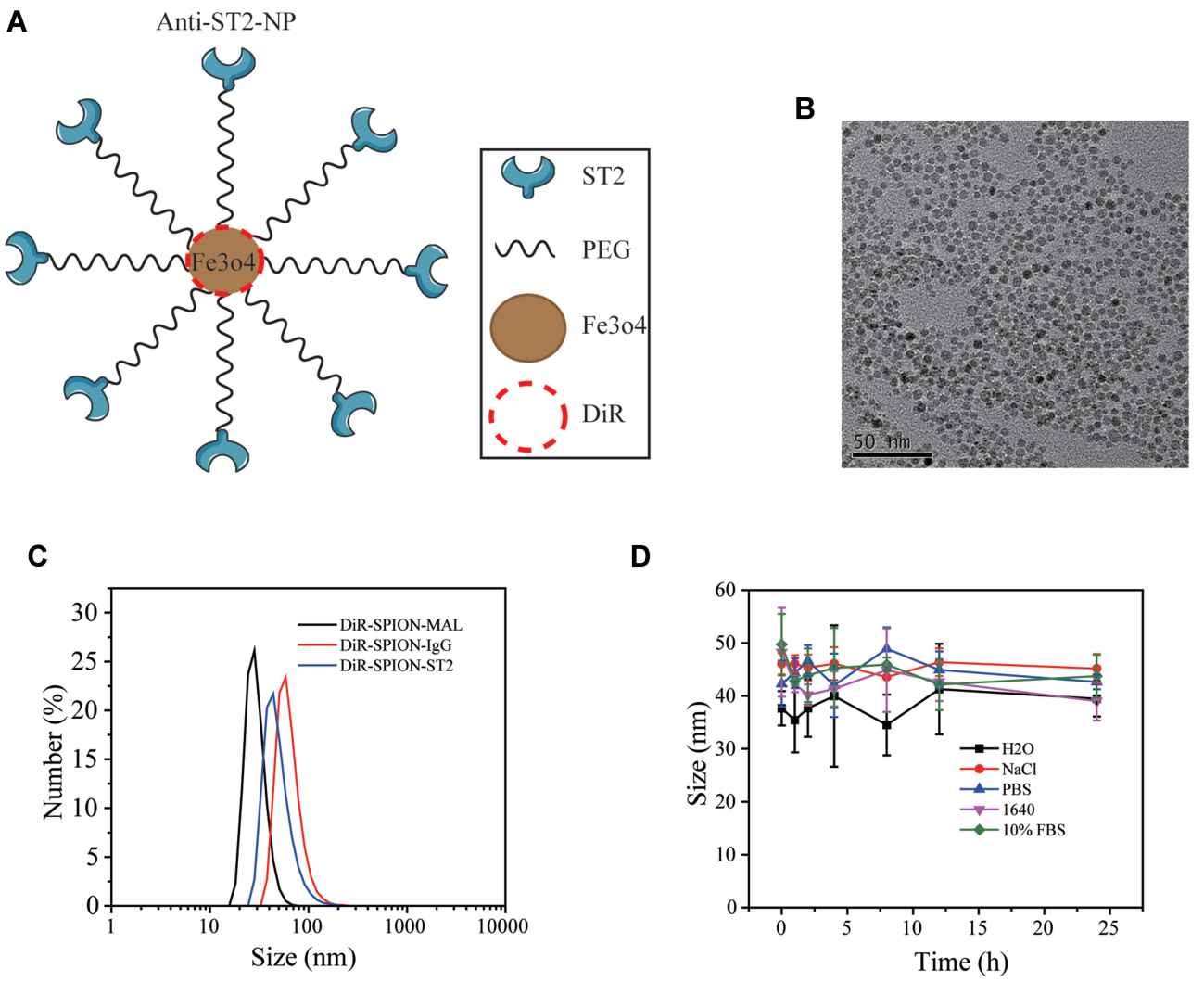

Figure 5 Characterization of DiR-SPIO-ST2-NP. (**A**) A diagram representing the synthetized DiR-SPIO-ST2-NP. (**B**) TEM images indicated that the DiR-SPIO-NPs were core-shell spherical nanoparticles. (**C**) The PDI of the nanoparticles. (**D**) Size distribution of the nanoparticles in different media.

Increased OVA-IgE in OVA-induced mice also indicated the successful establishment of the model. The positive correlation between ST2 and OVA-IgE support our hypothesis that airway inflammation can be alleviated by blocking ST2. Previous studies have reported that the IL-33 amplifies IgE synthesis and triggers anaphylaxis in naïve mice via ST2.[18] The positive correlation between ST2 and ILC2s is also consistent with the results in asthmatic patients. Numerous studies have proven that ILC2s promote $CD4^{+}$T cell participation in the development of asthma, influenza-induced lung inflammation and helminthic infection.[19] Our results also showed increased levels of $CD4^{+}$T cells in lung tissue of OVA-induced mice compared with naïve mice, which also correlated with ILC2s (Figure 4H–J).

Airway humidity, geometry, Specific defense mechanisms in the pulmonary epithelium and lungs, such as mucociliary escalators, macrophages, and enzyme activity, are challenges for ST2 delivery to the airway. Although several strategies for delivery have been formulated, there is still an urgent need to improve delivery efficiency and target specificity and reduce side effects. Nanoparticle-based lung targeting delivery systems have many advantages, including decreased mucociliary clearance, increased retention in the lungs, and biodegradability.[20] Previous studies have reported that various formulations of SPION have already been proven by the US Food and Drug Administration (FDA) as the magnetic resonance (MR) contrast agents for clinical use.[21] Thus their magnetic properties allow their quantitative biodistribution to be monitored in the target tissue using noninvasive MRI. In our present study, we conjugated DiR into SPION-NPs, which can be used to verify the delivery efficiency via FASC. Moreover, PEG

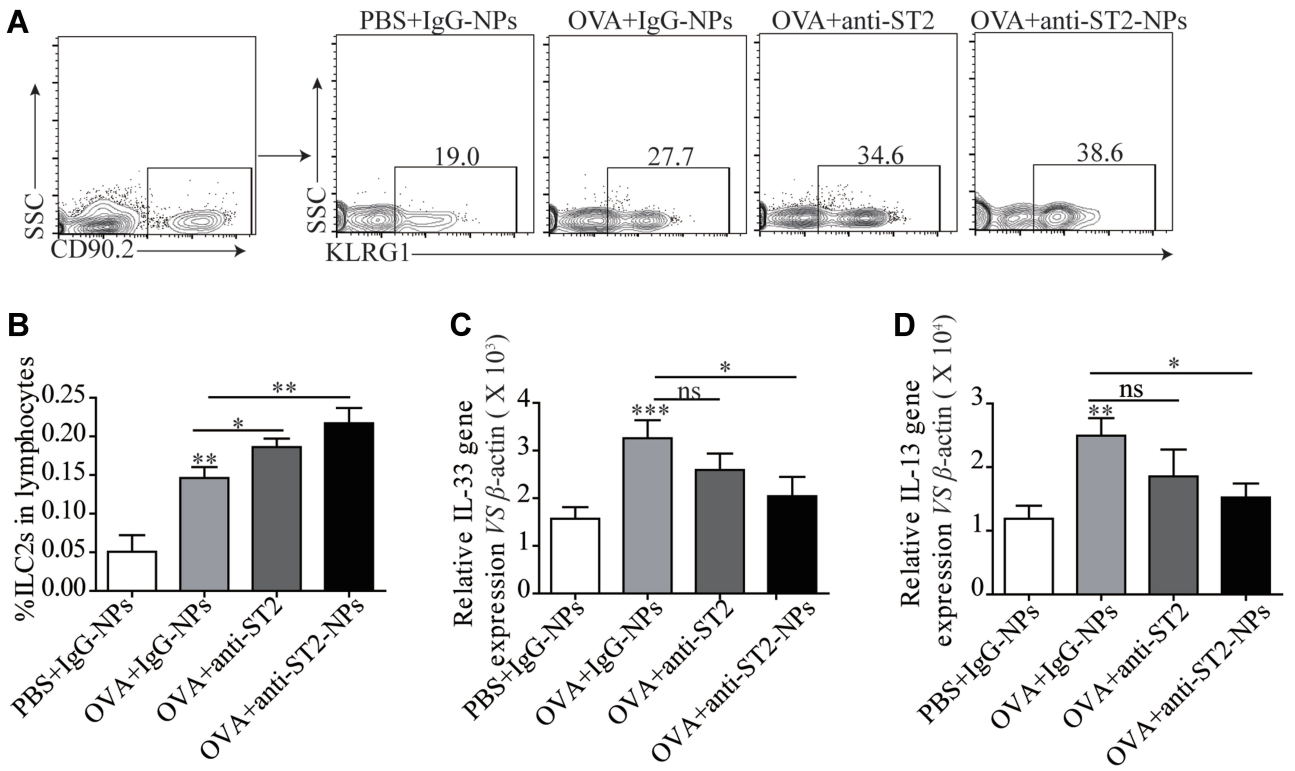

Figure 6 ILC2s were elevated in lung tissue after treated with anti-ST2-NPs. (**A**) Representative diagrams of flow cytometry analysis of the percentages of ILC2s in the lung of different groups. (**B**) Percentage of ILC2s in different groups of mice lung. RT-PCR results of the relative expression of IL-33 (**C**) and IL-13 (**D**) in mice lung tissue. Data are presented as mean ± SD, *P < 0.05; **P < 0.01; ***p<0.001 compared with control.

can prevent detection by the immune system and acts as a pH-sensor, which insures that it will dissociate in the acidic environment of inflamed tissues (pH = 6.4–6.8),[22] then the associated blocking antibodies will be released into the inflamed tissue.[9] These features lead to the more efficient and sustainable accumulation of anti-ST2 NPs in the airway and lung tissues. Figure 5 also demonstrated that the nanobubbles prepared in this study are stable and uniform even in different media.

PEG-coated NPs have strong ability to cross biological barriers, such as epithelial cells, and escape phagocytosis by immune cells.[23] As expected, delivery efficiency was aided by the expression of DiR (Figure 1B). Blocking ST2 may provide a new therapeutic strategy for patients with asthma. In the present study, we demonstrated that the OVA-induced increase in inflammatory cells in the airway was markedly reduced in OVA-induced mice treated with anti-IL4Rα, indicating that blocking ST2 is important for the influx of these inflammatory cells. Of note, anti-ST2-NPs more efficiently controlled OVA-induced lung inflammation, and anti-IgG1-NPs had neither immunogenic nor suppressive effects (Figure 1C).

Several studies have reported that ILC2s were increased in asthma patients and allergic asthma models.[15] During allergic sensitization, ILC2s can be activated by IL-33, resulting in priming of T cells and the production of IL-13 and IL-5. In our study, although anti-ST2-NPs treatment before OVA stimulation resulted in diminished inflammatory attraction to the airways, increased numbers of ILC2s with less IL-13 production were found in lung tissue (Figure 6B and D). We hypothesized that anti-ST2-NPs block the receptors in ILC2s, resulting a large number of anergic ILC2s that cannot be activated by IL-33 and leading to increased ILC2 levels as a compensatory mechanism (Figure 6A and B). Reduced IL-33 levels may be due to reduced inflammation (Figure 6C). Although ST2 is also expressed constitutively and stably on the surface of $CD4^+$T cells, especially on T helper type 2 (Th2) cells but not on Th1 cells, this study has demonstrated that ST2 does not play a critical role in Th2 cell development and function. $ST2^{-/-}$mice exhibited normal Th2 responses after infection with the helminthic parasite *Nippostrongylus brasiliensis* and in a mouse model of allergen-induced airway inflammation, and naïve $CD4^+$T cells isolated from $ST2^{-/-}$ mice can also develop into Th2 cells in response to IL-4 in vitro.[24] However, our data showed reduced $CD4^+$T cells in OVA-

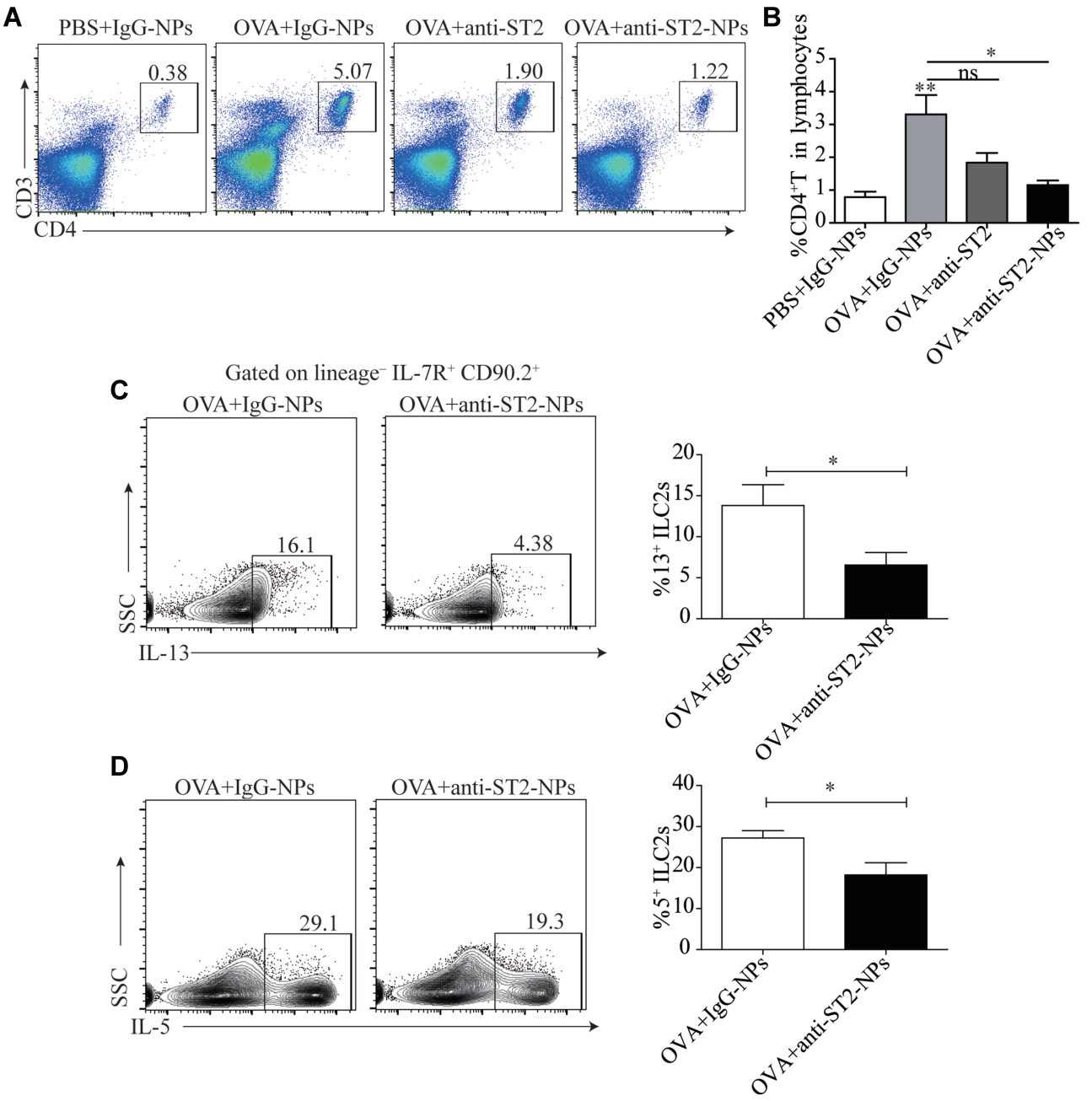

Figure 7 Airway inflammation is alleviated by anti-ST2-NPs that target the ILC2s-CD4+T axis. (**A**) Representative diagrams of flow cytometry analysis of the percentages of $CD4^+$T cells in the lung of different groups. (**B**) Frequencies (n = 8) of percentage of $CD4^+$T cells in mice lung in different groups of mice lung. Flow cytometry evaluated the expression of IL-13 (**C**) and (**D**) on ILC2s in vivo. Data are presented as mean ± SD, *P < 0.05; **P < 0.01 compared with control.

induced mice lung tissues treated with anti-ST2-NPs (Figure 7A and B). A previous study reported that ILC2s and T cells cooperate through MHCII-dependent activation to potentiate the type-2 response,[25] and IL-13 from ILC2s promote DC migration to the draining lymph nodes to stimulate $CD4^+$T cell polarization.[26] Then, we detected IL-13 and IL-5 secreted by ILC2s in OVA-induced mice with or without anti-ST2-NP treatment, and our results showed less IL-13 and IL-5 in ILC2s from OVA-induced mice treated with anti-ST2-NPs (Figure 7C and D). We think that this effect may be caused by those anergic ILC2s and subsequent reductions in $CD4^+$T cells, which further relive allergic lung inflammation in an OVA-induced asthma model.

In summary, in the present study, we demonstrated that OVA-induced lung inflammation could be controlled by anti-ST2-NP treatment by blocking ST2 expression in ILC2s and subsequently reducing the number of CD4+T cells due to reduced production of IL-13 and IL-5. Our study also

demonstrated that the nanoparticle delivery system could improve the performance of anti-ST2, which may be used as a strategic tool to expand current drug markets.

Data Sharing Statement

The data used to support the findings of this study are included within the article.

Acknowledgments

This work was supported by grants from the National Natural Science Foundation of China (grant 81801568), the National Science Foundation for Post-doctoral Scientists of China (grant 2018M642314), the Postdoctoral Science Foundation of Jiangsu Province (grant 2018K235C), the Young Talent Development Plan of Changzhou Health Commission (grant CZQM2020009), and the Changzhou Science and Technology Project (Applied Based Research, No. CJ20180035).

Disclosure

The authors report no conflicts of interest in this work.

References

1. Phan HT, Vu GV, Vu GT, et al. Global mapping of research trends on interventions to improve health-related quality of life in asthma patients. *Int J Environ Res Public Health*. 2020;17(10):10. doi:10.3390/ijerph17103540
2. Gorczynski RM, Maqbool T, Hoffmann G. Mechanism(s) of prolonged attenuation of allergic responses after modulation of idiotypic regulatory network. *Allergy Asthma Clin Immunol*. 2019;15(1):79. doi:10.1186/s13223-019-0393-7
3. Fitzpatrick AM, Chipps BE, Holguin F, Woodruff PG. T2-"low" asthma: overview and management strategies. *J Allergy Clin Immunol Pract*. 2020;8(2):452–463. doi:10.1016/j.jaip.2019.11.006
4. Peters MC, Ringel L, Dyjack N, et al. A transcriptomic method to determine airway immune dysfunction in T2-high and T2-low asthma. *Am J Respir Crit Care Med*. 2019;199(4):465–477. doi:10.1164/rccm.201807-1291OC
5. Ridolo E, Pucciarini F, Nizi MC, et al. Mabs for treating asthma: omalizumab, mepolizumab, reslizumab, benralizumab, dupilumab. *Hum Vaccin Immunother*. 2020;1–8.
6. Nagasawa M, Heesters BA, Kradolfer CMA, et al. KLRG1 and NKp46 discriminate subpopulations of human CD117(+)CRTH2(-) ILCs biased toward ILC2 or ILC3. *J Exp Med*. 2019;216(8):1762–1776. doi:10.1084/jem.20190490
7. Barlow JL, Peel S, Fox J, et al. IL-33 is more potent than IL-25 in provoking IL-13-producing nuocytes (type 2 innate lymphoid cells) and airway contraction. *J Allergy Clin Immunol*. 2013;132(4):933–941. doi:10.1016/j.jaci.2013.05.012
8. Frisbee AL, Saleh MM, Young MK, et al. IL-33 drives group 2 innate lymphoid cell-mediated protection during clostridium difficile infection. *Nat Commun*. 2019;10(1):2712. doi:10.1038/s41467-019-10733-9
9. Al Faraj A, Shaik AS, Afzal S, Al-Muhsen S, Halwani R. Specific targeting and noninvasive magnetic resonance imaging of an asthma biomarker in the lung using polyethylene glycol functionalized magnetic nanocarriers. *Contrast Media Mol Imaging*. 2016;11(3):172–183. doi:10.1002/cmmi.1678
10. Luo B, Zhang H, Liu X, Rao R, Wu Y, Liu W. Novel DiR and SPIO nanoparticles embedded PEG-PLGA nanobubbles as a multimodal imaging contrast agent. *Biomed Mater Eng*. 2015;26(Suppl 1):S911–916.
11. Song X, Gong H, Yin S, et al. Ultra-small iron oxide doped polypyrrole nanoparticles for in vivo multimodal imaging guided photothermal therapy. *Adv Funct Mater*. 2014;24(9):1194–1201. doi:10.1002/adfm.201302463
12. MacArthur Clark JA, Sun D. Guidelines for the ethical review of laboratory animal welfare People's Republic of China national standard GB/T 35892-2018 [issued 6 February 2018 effective from 1 September 2018]. *Allergy Asthma Clin Immunol*. 2020;3(1):103–113. doi:10.1002/ame2.12111
13. Myou S, Leff AR, Myo S, et al. Blockade of inflammation and airway hyperresponsiveness in immune-sensitized mice by dominant-negative phosphoinositide 3-kinase-TAT. *J Exp Med*. 2003;198(10):1573–1582. doi:10.1084/jem.20030298
14. Verma M, Liu S, Michalec L, Sripada A, Gorska MM, Alam R. Experimental asthma persists in IL-33 receptor knockout mice because of the emergence of thymic stromal lymphopoietin-driven IL-9(+) and IL-13(+) type 2 innate lymphoid cell subpopulations. *J Allergy Clin Immunol*. 2018;142(3):793–803.e798. doi:10.1016/j.jaci.2017.10.020
15. Pasha MA, Patel G, Hopp R, Yang Q. Role of innate lymphoid cells in allergic diseases. *Allergy Asthma Proc*. 2019;40(3):138–145.
16. Yu QN, Guo YB, Li X, et al. ILC2 frequency and activity are inhibited by glucocorticoid treatment via STAT pathway in patients with asthma. *Allergy*. 2018;73(9):1860–1870. doi:10.1111/all.13438
17. Ying X, Su Z, Bie Q, et al. Synergistically increased ILC2 and Th9 cells in lung tissue jointly promote the pathological process of asthma in mice. *Mol Med Rep*. 2016;13(6):5230–5240. doi:10.3892/mmr.2016.5174
18. Komai-Koma M, Brombacher F, Pushparaj PN, et al. Interleukin-33 amplifies IgE synthesis and triggers mast cell degranulation via interleukin-4 in naïve mice. *Allergy*. 2012;67(9):1118–1126. doi:10.1111/j.1398-9995.2012.02859.x
19. Han X, Bai S, Cui Y, Zhu W, Zhao N, Liu B. Essential role of CD4(+) T cells for the activation of group 2 innate lymphoid cells during respiratory syncytial virus infection in mice. *Immunotherapy*. 2019;11(15):1303–1313. doi:10.2217/imt-2019-0084
20. McDaniel DK, Ringel-Scaia VM, Coutermarsh-Ott SL, Allen IC. Utilizing the lung as a model to study nanoparticle-based drug delivery systems. *Methods Mol Biol*. 2018;1831:179–190.
21. Mahmoudi M, Sahraian MA, Shokrgozar MA, Laurent S. Superparamagnetic iron oxide nanoparticles: promises for diagnosis and treatment of multiple sclerosis. *ACS Chem Neurosci*. 2011;2(3):118–140. doi:10.1021/cn100100e
22. Tsuchiya H, Mizogami M, Ueno T, Takakura K. Interaction of local anaesthetics with lipid membranes under inflammatory acidic conditions. *Inflammopharmacology*. 2007;15(4):164–170. doi:10.1007/s10787-007-1601-5
23. Lin YL, Huang XF, Chang KF, Liao KW, Tsai NM. Encapsulated n-butylidenephthalide efficiently crosses the blood-brain barrier and suppresses growth of glioblastoma. *Int J Nanomedicine*. 2020;15:749–760. doi:10.2147/IJN.S235815
24. Hoshino K, Kashiwamura S, Kuribayashi K, et al. The absence of interleukin 1 receptor-related T1/ST2 does not affect T helper cell type 2 development and its effector function. *J Exp Med*. 1999;190(10):1541–1548. doi:10.1084/jem.190.10.1541
25. Oliphant CJ, Hwang YY, Walker JA, et al. MHCII-mediated dialog between group 2 innate lymphoid cells and CD4(+) T cells potentiates type 2 immunity and promotes parasitic helminth expulsion. *Immunity*. 2014;41(2):283–295. doi:10.1016/j.immuni.2014.06.016
26. Halim TY, Steer CA, Mathä L, et al. Group 2 innate lymphoid cells are critical for the initiation of adaptive T helper 2 cell-mediated allergic lung inflammation. *Immunity*. 2014;40(3):425–435. doi:10.1016/j.immuni.2014.01.011